ARAI Journal of Mobility Technology
Volume 1 • Issue 1 • October–December, 2021, pp. 69-76
Research Paper
https://doi.org/10.37285/ajmt.1.0.9

# A Systematic Approach to Evaluation of Various Cooling Strategies for EV Battery Pack Prismatic Cell using Analytical and Numerical Methods

**P. D. Yogesh, Vivek Anami and Yogesh Jaju**

*TataTechnologies Ltd., Plot No 25, Phase 1, Hinjewadi Rajiv Gandhi Infotech Park, Hinjawadi, Pune, Maharashtra, India - 411057*

**ABSTRACT**

Technology to maximize energy density and life of Lithium-ion batteries at a gradually reducing cost is evolving day by day. Fast charging of the battery pack has become one of the major requirements of electric vehicles. Such a requirement invariably poses certain challenges to the cells of the EV battery pack. One of them is to achieve an efficient and an optimal thermal management of the battery pack to maintain uniform operating temperature of the cells and within the manufacturers' allowable range to ultimately increase the lifespan and reliability of the battery pack. The current work discusses the design strategies of cell cooling, heat load estimation & features of different cooling strategies. A MS Excel spreadsheet-based design tool was developed to quickly estimate the cell temperature gradient. The results from the spreadsheet-based tool, which was based on fundamental equations, correlated well with 3D CFD simulation results. The results were analysed and the cooling strategy for the battery pack was decided based on the analytical and numerical values obtained from the analysis of various cell parameters.

**KEYWORDS:** Thermal management; Design strategies of cell cooling; Heat load estimation; Spread sheet; Temperature gradient; 3D CFD simulation.

## Introduction

Lithium-ion cells are nowadays viewed as the most promising advanced battery cell technology for the next-generation electric and hybrid electric vehicles (EVs and HEVs). These cells are well-known for their high energy and power densities, high operating voltage and discharge rate, short charging time and long cycle life apart from offering us the clean and green mode of transport.

Despite these positive aspects that justify the recent spread of this technology, it is evident that under high discharge conditions, which involve high rates of Joule anheat generation and exothermic electrochemical reactions, batteries are prone to an excessive temperature rise that can initiate swelling, thermal runaway, electrolyte fire, and in extreme cases, potential explosion as well. Thus, it is imperative that lithium-ion batteries must be carefully monitored and managed (electrically and thermally) to avoid problems related to safety and performance. For these reasons, the battery temperature should be maintained within a temperature range that is considered optimum in order to achieve good performance and long life, both for use and storage. A typical safe operating temperature range for lithium-ion batteries is between 20°C and 40°C[1].

The battery cooling can be categorized as active cooling and passive cooling. Table-1 lists popular HEV and EV vehicles and the cooling system they deploy for battery cooling. In Nissan-Leaf, the battery cooling is based on the radiation (passive) cooling principle. In this system, the battery is cooled by radiating heat to the car's interior and exterior. The cooling performance to large extent depends upon ambient temperature. This technology is not suitable for Indian climate conditions, which are not only extreme but vary significantly from region to region Active cooling concepts are categorized as a) Air cooling b) Liquid Cooling & c) Refrigerant Cooling. Air is not a good conductor of heat and so, air cooling is used in HEVs where the heat load on the battery is comparatively lower. Liquids and refrigerants are good conductors of heat. Liquid and refrigerant cooling systems are used in EVs where the heat load in the battery is relatively high. The refrigerant cooling system is a complex system as it is challenging to control the flow of the refrigerant. Liquid cooling is widely used in the EVs and is mostly preferred.

**ABBREVIATIONS:** 3D – 3 Dimension; CFD– Computational Fluid Dynamics; EV – Electric Vehicle; HEV – Hybrid Electric Vehicle; Max – Maximum; 1D – 1 Dimension; H – Height; W – Weight; T– Thickness; HTC – Heat Transfer Coefficient; PCM – Polymer Matrix Composite; ECM–Equivalent Circuit Model; LFP – Lithium-ion Phosphate; Q – Cell heat source; q – Volumetric heat source; k – Cell conductivity; L– Cell normal distance; mm – millimeter; LI-ion – Lithium-ion.

TABLE 1
EVs/HEVs and their cooling system.

| Vehicle | Cooling Type |
|---|---|
| Nissan Leaf | Passive (Radiation) |
| Toyota Prius | Active (Air) |
| Tesla | Active (Liquid) |
| BMW i3 | Active (Refrigerant) |

## Methodology

Figure-1 shows the methodology followed while deciding the cooling strategy for the prismatic cells.

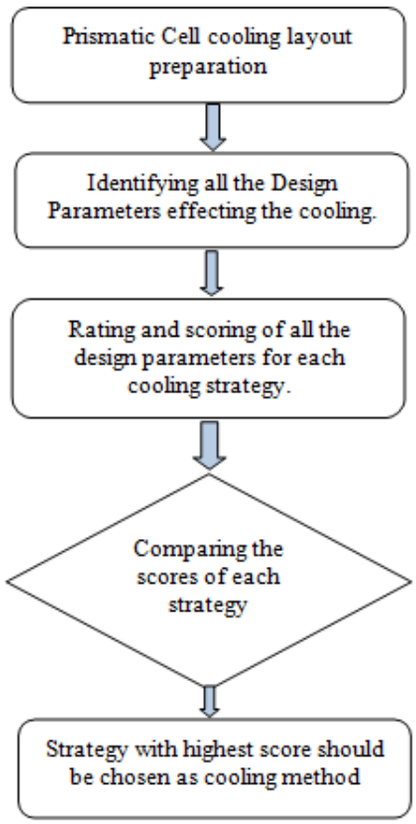


**Fig. 1.** Cooling strategy decision process.

### Cell Cooling Strategies

Cells are primarily cooled by a cooling plate. In the cooling plate, there are cooling channels through which the liquid coolant (Water + Glycol) at low temperature is circulated. The cells are not directly connected to the cooling plate; rather, a thermal pad is sandwiched between the cells and the cooling plate. The pad is thermally conductive and sticky in nature. Due to proper adherence of the pad with the cell and the cooling plate, a "thermal contact" is established between them. The battery cells have two types of casing: a) pouch b) hard casing. The prismatic and cylindrical cells have a hard casing while the pouch cells are flexible in nature. When cell pouches are used in an EV battery pack, they need an appropriate frame structure to hold the cell pouches together. We considered the prismatic cells in the current battery pack cooling strategy design.

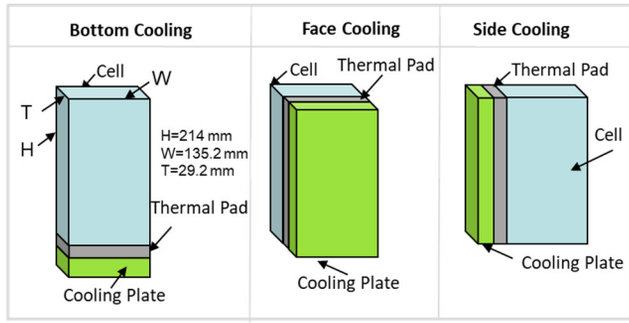


**Fig. 2.** Representation of bottom, face and side cooling arrangement.

Based on the cooling plate location, we categorized the battery cooling system as 1)Bottom cooling 2)Face cooling 3)Side cooling as shown in Figure-2. Each cooling strategy has its own advantages and disadvantages.

In a battery pack, the cell temperature depends upon multiple parameters such as 1) Amount of cell surface area exposed to the cooling system 2) Cooling channel design 3) Coolant inlet conditions4) thermal pad properties 5)Cell conductivity6) Volumetric heat source 7) Cell normal distance from cooling channel (L). 8) Bus bar location &overall arrangement of the cooling system. Many of these parameters are interdependent! To evaluate the effect of different parameters, a 3D CFD simulation was performed. For the current battery pack, following temperature targets were set at cell and at pack levels:

- Max. temperature for the pack: <= 32 °C.
- Max. temperature gradient within cell: <=1.5°C.

Keeping tight control over the cell to cell temperature variation is important as it offers a buffer to the variation in temperature in actual operating conditions. The battery when operated between 15 °C to 35 °C gives best life and performance[2]. The 3D CFD simulation can predict the temperatures at cell and pack levels. The battery supplier has multiple cell configurations with different capacities and dimensions. Evaluating the different cells for thermal performance using 3D CFD simulation is not always feasible. To attenuate this problem, we developed an MS Excel spreadsheet based 1D temperature estimation tool to quickly estimate the temperature gradient in the cell. This tool was of great benefit in the sense it averted redundant 3D CFD simulations while offering insights into the various designs with a reasonable reliability. Initial battery design evaluation and data analysis was done using 3D CFD approach. The information obtained from the 3D simulation was subsequently used in the 1D tool, which was used to evaluate different cells from the supplier. The results obtained from 3D and 1D simulations were used to rate the parameters in the decision matrix for cooling system strategy selection. The detailed decision matrix is discussed in subsequent section.

### Area of cooling

The cell area exposed to the cooling system is one of the important factors that affect the final cell temperature. Table-2 gives the cell surface area available

for cooling for different cooling strategies. As shown in Figure-2, the face cooling approach offers maximum cell surface area, i.e., (214*135.2=28933 mm$^2$) largest area is exposed to the cooling plate. For example, Chevy Volt by General Motors uses a face cooling approach. While the face cooling system is the most effective system to cool the battery cell, EVs do deploy the base plate cooling concept as well, depending upon cell size and to trade-off on associated complexity.

TABLE 2

Surface area available for cooling.

| Cooling strategy | Cell Surface Area (mm$^2$) |
|---|---|
| Bottom Cooling (T*W) | 3948 |
| Face Cooling (W*H) | 28933 |
| Side Cooling (T*H) | 6249 |

## Cooling Channel Design

As mentioned earlier, the cell face is cooled by the cooling plate through which water and glycol mixture is circulated. A cooling plate of suitable dimensions (H=180 mm, W=1357 mm & T=8mm) was designed. Multiple cooling plate design strategies can be used for the Battery pack cooling system design. Three strategies (U-channel, S-channel& W-channel) for side cooling are shown in Figure-3. The inlet channel is given near to cell terminal at which, maximum heat is generated. The outlet is given at the cell bottom, where less heat is generated.

As the number of paths in the cooling channel increases, the velocity/HTC(heat transfer coefficient) of cooling fluid increases, but at the same time, pressure drop also increases as shown in Figure-4. The U-shaped design has the least pressure drop and the W-shaped design has the highest pressure drop. The S-shaped design has an inlet and outlet in opposite directions that makes routing of the tube more difficult. The design with the least pressure drop (U-channel) performs better and is recommended.

## Coolant Inlet Condition

At the cooling channel inlet, coolant mass flowrate and coolant temperature are two important parameters that decide the cell temperature. Coolant mass flow depends upon the cooling channel system resistance and coolant pump flow capacity. To estimate the coolant flow, system resistance concept as shown in Figure-5 was used. The intersection of system resistance and pump characteristics provides an estimate of mass flow required through the cooling system. The mass flow we got through this method is total mass flow through the system. The battery pack has multiple parallel paths to cool individual modules and cells. The design ensures coolant flow per cell is the same.

Figure-6 shows the relation between the coolant mass flow rate (module-level) and the cell temperature. As obvious, the relationship is not linear. Beyond a limit, any further increase in the mass flow rate does not help reducing the cell temperature in the same proportion as the relationship becomes asymptotic in nature.

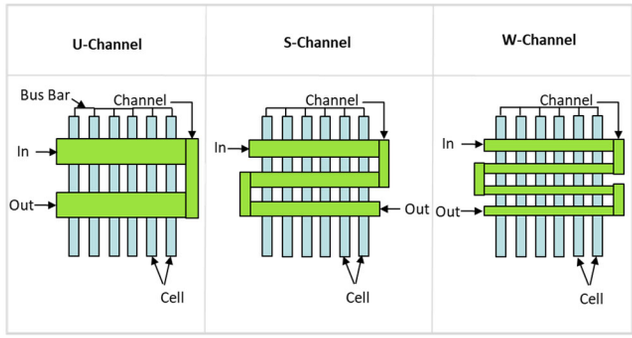


**Fig. 3.** U-channel S-channel W-channel cooling strategy.

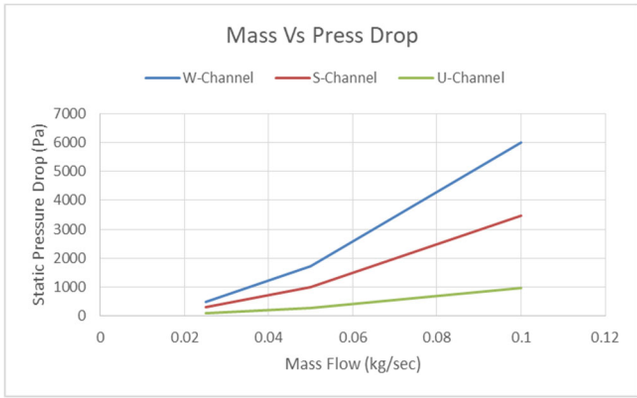


**Fig. 4.** Mass Vs Pressure drop chart.

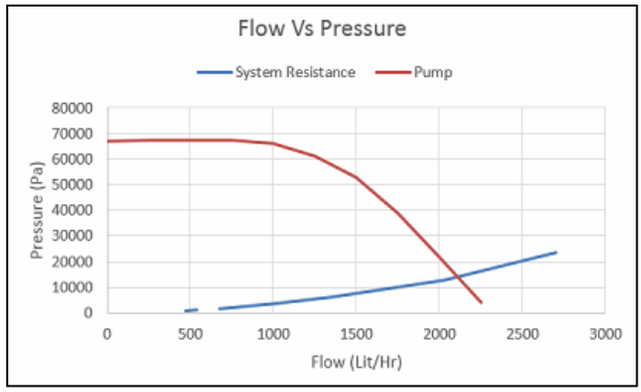


**Fig. 5.** Mass Flow Vs Pressure graph.

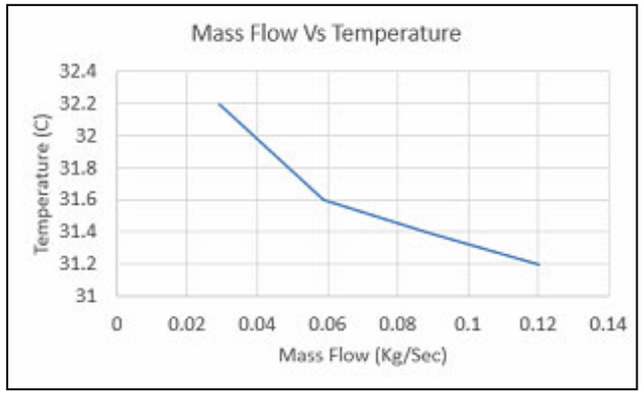


**Fig. 6.** Mass flow Vs Temperature graph.

There is an inherent disadvantage of increasing the coolant flow rate beyond a limit. The pressure drop in the system increases exponentially with an increase in the mass flow rate as shown in Figure-7

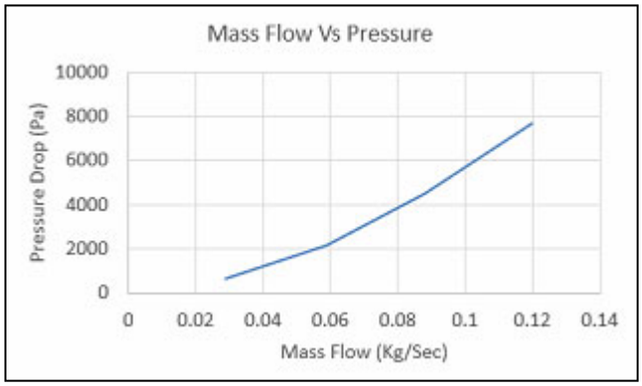


**Fig. 7.** Mass flow Vs Pressure graph.

Figure-8 shows the linear relationship between the coolant temperature and the cell maximum temperature. As the coolant inlet temperature is reduced, the cell temperature reduces proportionally. Thus, in order to maintain the desired cell temperature, it is more beneficial to reduce coolant inlet temperature than increasing the coolant flow rate.

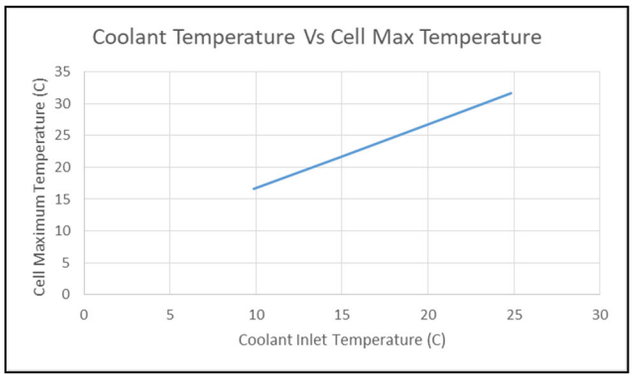


**Fig.8.** Coolant Temperature Vs Cell Max Temperature graph.

As the coolant inlet temperature is reduced, the cell temperature gradient remains the same.

For one module consisting of 36 cells, a mass flow of 0.059 kg/sec at 25 °C temperature was given as an input condition for simulation. The coolant inlet temperature and mass flow rate depend upon the external cooling loop and were maintained at fixed values during the evaluation of the different strategies and not included in the decision matrix for the battery pack.

### The Thermal Pad Properties

As mentioned earlier, the thermal pad ensures positive contact between cells and the cooling plate. The pads with different materials like PCM-based phase change, silicon-based, etc., are available. The silicon pad comes in standard thicknesses such as 1 mm, 2 mm, 4mm, etc. A pad with 2 mm thickness is good for battery packaging. The silicon pad comes with different grades, which have different thermal properties. As per material grade, the conductivity of the pad can vary from 0.7 upto3W/m²/K. Different pads with different conductivity were evaluated and cell maximum temperature was estimated. The results are shown in Figure-9. It was observed that as thermal conductivity increases, the drop in the cell temperature becomes asymptotic in nature. The governing heat transfer equation (1) is given below:

$$Q = k \times A \times \frac{(T1-T2)}{dx} \quad .....(1)$$

The heat generated Qin the cell is fixed. The coolant inlet temperature (T2=25°C) does not change much in the cooling channel and can be assumed fixed. If we increase the thermal pad conductivity, the cell temperature (T1) does not reduce much and the relationship becomes asymptotic.

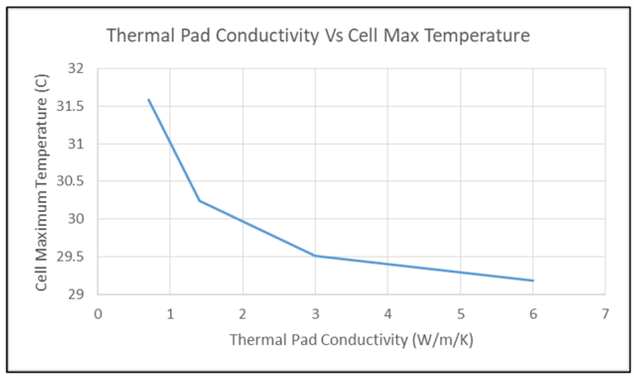


**Fig. 9.** Thermal Pad conductivity Vs Cell Max Temperature.

The cost of the pad is exponentially higher with the rise in conductivity as shown in Figure-10. The pad with the lowest conductivity (0.7 W/m²/K) and with 2mm thickness can be used at the initial design stage as it is cost effective. Pad with higher conductivity can be used if temperature targets are not met. The thermal pad used in the three cooling strategies was the same and not considered as a variable parameter for the decision matrix.

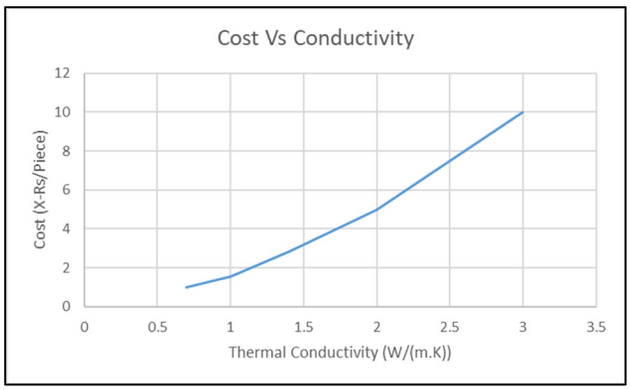


**Fig. 10.** Cost Vs Conductivity of thermal pad.

### Cell Conductivity

Cell conductivity is also one of the important factors for deciding the cooling strategy. The cell has anisotropic thermal conductivity. The conductivity is higher in the planar direction and while it is lower in the transverse direction as shown in Figure-11.Higher the conductivity

of the cell, better is the heat transfer and better is the cell cooling.

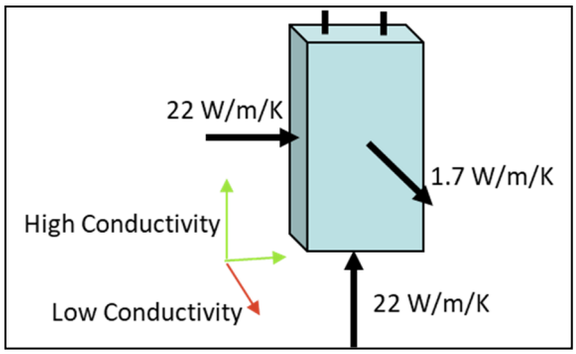


**Fig. 11.** Cell conductivity in different directions.

### Volumetric Heat Generation

Every battery pack cell has its own internal resistance. When current flows in the cell, heat is generated in the cell and the cell temperature increases. There are multiple ways to model cell heat generation; for example, simple resistance model, ECM, etc. We used a simple resistance model for cell internal heat generation for the LFP chemistry cells we chose. The internal resistance of the cell for LFP chemistry is in the range of 0.5 mΩ to 1 mΩ. The heat generated inside the cell is the same for three cooling strategies and not considered as a variable parameter for the decision matrix. The cell heat generated is given by the equation (2) given below

$$Q = 1.1 \times I^2 \times R \quad \text{.....(2)}$$

$$Q = 1.1 \times 50^2 \times 0.001 = 2.75\ Watt$$

Cell volume is given by equation (3) given below

$$CellVolume = H \times W \times T \quad \text{.....(3)}$$

$$CellVolume = 0.215 \times 0.135 \times 0.0292$$

$$= 0.00085\ m^3$$

Heat per unit volume is given by the equation (4) given below

$$q = \frac{Q}{Volume} \quad \text{.....(4)}$$

$$q = 2.75 \div 0.00085 = 3244.7\ Watt/m^3$$

### Cell Normal Distance

Cell normal distance as shown in Figure-12 greatly affects the temperature gradient in the cell. For a given heat generation in the cell, if the cell size (cell normal distance) changes the temperature gradient in the cell changes. Smaller the cell normal distance, lesser is the temperature gradient.

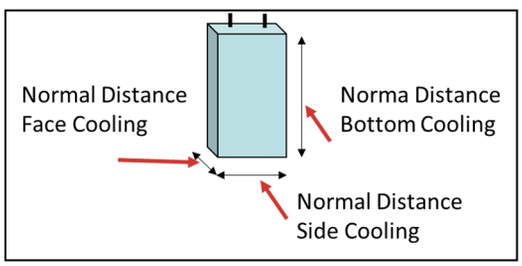


**Fig. 12.** Cell normal distance.

For the same cell, two cooling cell strategies were evaluated. For bottom cooling strategy (Strategy-A) the cell normal distance is 214 mm. For side cooling strategy (Strategy-B) the cell normal distance is 135 mm. It was observed that Strategy-A resulted into both higher absolute temperature and temperature gradient as compared to Strategy-B. A comparison of the results of the two strategies is shown in Table 3.

TABLE 3

Max temperature and temperature gradient of different strategies of cell.

| Strategy | Temperature Max(C) | Temperature Gradient (C) |
|---|---|---|
| A | 31.4 | 3.38 |
| B | 29 | 1.57 |

In the early development stage, the cell temperatures and cell temperature gradients were estimated with 3D CFD simulation. The next section discusses the CFD simulation and results.

### CFD Simulation

Bottom cooling and side cooling strategies were evaluated by means of 3D CFD simulation. Following boundary conditions used for thermal simulation:

- coolant inlet mass flow rate = 0.059 kg/sec.
- coolant inlet temperature = 25 °C.
- heat flux = 2.75 Watt (3244 Watt/m$^3$) on each cell.

A thermal pad of 2mm thickness was used in between cells and the cooling plates. Table-4showsthe properties of different battery components. The coolant in the system was a water and glycol mixture (50:50).

The thermal conductivity of the mixture is 0.3 W/m/K which is less than pure water. Following cell temperature targets were set after discussion with the supplier:

1) Max temperature target for the cell: 32 °C.
2) Max temperature gradient within the cell: 1.5 °C.
3) Temperature gradient target (cell to cell) within the battery pack is 1.5 °C.

TABLE 4

Properties of battery components.

| Material | Density kg/m^3 | Specific Heat J/kg/k | Conductivity W/m/k |
|---|---|---|---|
| Cell | 1200 | 871 | In plane: 22<br>Out of plane : 1.7 |
| SiliconePad | 1200 | 871 | 0.7 |
| Water | 998.2 | 4182 | 0.3 |

As shown in Figures 13 & 14, it was found that:

1) The maximum temperature of the bottom cooling is 31.6 °C while that for the side cooling, it was 29 °C.
2) The temperature gradient is more (3.38 °C) for the bottom cooling as compared to the side cooling (1.57 °C). Thus, side cooling approach gets a better rating and score as compared to bottom cooling. It is important to note that although the maximum temperature for the bottom cooling concept is below the set temperature target limit, the temperature gradient in the cell exceeds the

target. The cell exceeds the temperature gradient limit by0.07 °C for the side cooling strategy.

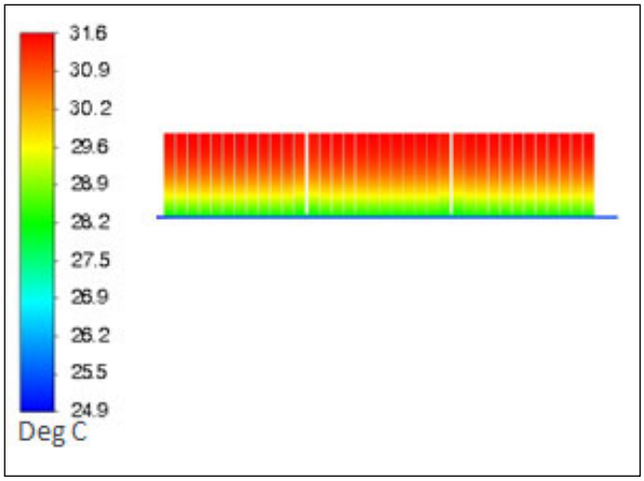


**Fig. 13**. Cell Temperature: Bottom Cooling Concept.

The difference in inlet& the outlet temperatures of the coolant is very small (of the order of 0.5 °C).The heat transfer equation (5) is given below.

Water has a very good thermal capacity (m*Cp) and this ensures the uniform cell temperature in the battery pack. For the current design configuration, a temperature gradient across the pack (cell to cell) of magnitude0.08°C was achieved.

$$Q = m \times C_p \times (T1 - T2) \quad \text{.....(5)}$$

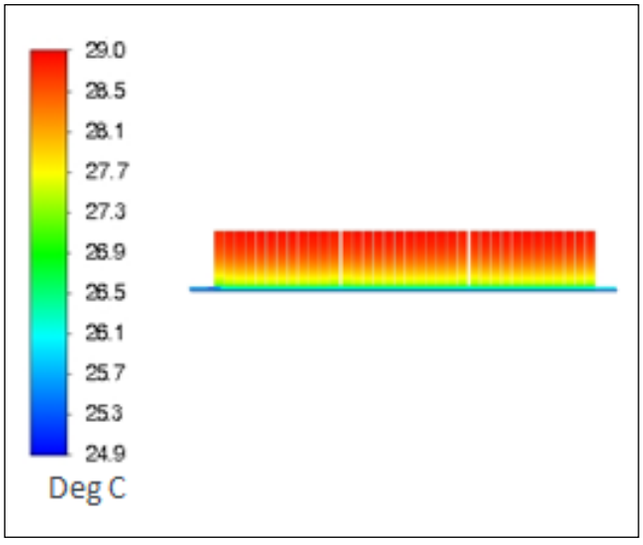


**Fig. 14.** Cell Temperature: Side Cooling Concept.

As mentioned in this section the cell temperature gradient was 1.57°C. The cell temperature gradient was marginally higher than the target but was within the acceptable tolerance limit. We analysed different cells from the supplier for the cell temperature gradient. The evaluation of the different cells for thermal performance in 3D simulation is not feasible. A spreadsheet-based 1D temperature estimation tool was developed. This offered a quick estimation of temperature gradient in the cell for different cell geometries thereby saving time and cost involved in the overall evaluation process.

The next section discusses in detail the 1D spreadsheet based tool.

### One dimensional tool

A MS Excel based spreadsheet tool was developed. The sheet requires three basic inputs like a) geometry b) cell volumetric heat source c) conductivity. Cell temperature and temperature gradient can be predicted with these basic parameters. The spreadsheet used an empirical equation (6) given below.

$$T_{max} = (q \div (8 \times k) \times (2 \times L)^2) + (celltemperatureatcoolingchannel) \text{.....(6)}$$

The first term on the right-hand side gives the temperature gradient. The second term on the right-hand side is the cell temperature near the cooling plate. This temperature is estimated from hand calculation or it can evaluated by CFD simulation. Once we estimated temperature at the wall the same can be used as a reference for evaluating different cells for maximum temperature and temperature gradient. The temperature gradient behaves independently of cell wall temperature near the cooling plate. The gradient depends upon the cell volumetric heat source (q), conductivity (k) and cell normal distance (L). The cell conductivity does not change much for a particular cell chemistry. The other two parameters cell heat source and normal distance varies with change in load current and cell dimension or design.Table-5gives the cell temperature gradient values (°C) for different cell heat sources (Watt) and cell normal distances (mm). This table is generated for the cell with dimensions as H=214mm, W=135.2mm T=29.2mmand with cell conductivity of 22 W/m/K.

TABLE 5

Cell normal distance vs cell temperature gradient.

| Cell Normal Distance (mm) | Heat Source 1.5 Watt | Heat Source 2.0 Watt | Heat Source 2.75 Watt |
|---|---|---|---|
| 0 | 0.000 | 0.000 | 0.000 |
| 20 | 0.016 | 0.022 | 0.030 |
| 40 | 0.065 | 0.086 | 0.118 |
| 60 | 0.145 | 0.194 | 0.266 |
| 80 | 0.258 | 0.344 | 0.473 |
| 100 | 0.404 | 0.538 | 0.740 |
| 120 | 0.581 | 0.775 | 1.065 |
| 140 | 0.791 | 1.055 | 1.450 |
| 160 | 1.033 | 1.377 | 1.894 |
| 180 | 1.307 | 1.743 | 2.397 |
| 200 | 1.614 | 2.152 | 2.959 |
| 214 | 1.848 | 2.464 | 3.388 |

Figure-15 shows the variation of the cell temperature gradient plot for different cell heat sources and cell normal distances. As mentioned earlier, the cell temperature gradient is a function of volumetric heat source (q), conductivity (k), and cell normal distance (L). The thermal conductivity for a given cell is constant. Plotting the temperature gradient with heat source (Q) and cell normal distance (L) helps more in the physical interpretation of the simulation data (Table 5) and 3D plot.

Brown area show cells below 1°C temperature gradient can have a normal distance of 120mm, whereas the grey area show cell below 1.5°C temperature gradient can have normal distance around 140mm.

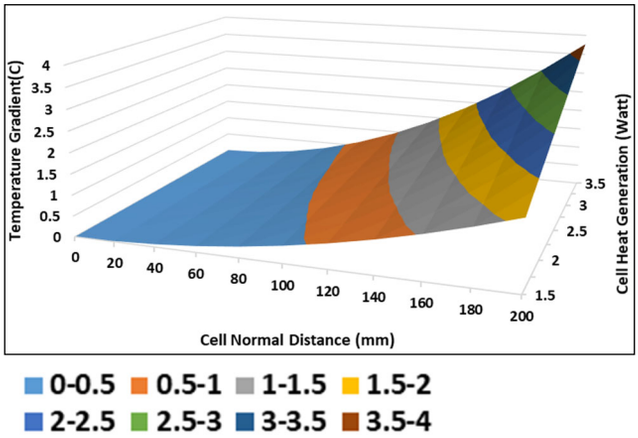


**Fig.15.** 3D graph Normal distance Vs Heat generated VsTemperature.

A sectional plot gives better insight into the thermal gradient behaviour of the cell. Figure-16 shows the cut section plot of the 3D surface at a constant heat source (2.77 Watt).

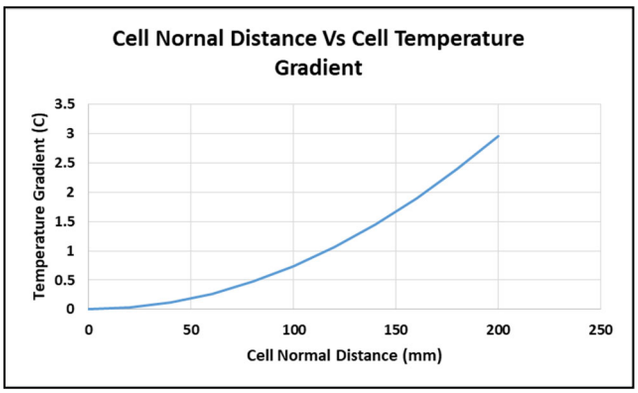


**Fig. 16.** Cell Normal Distance Vs Cell Temperature Gradient for bottom cooling

To achieve the cell temperature gradient below 1.5 °C the cell normal distance should be less than 140 mm while for the gradient to be less than 1 °C, the cell normal distance should be less than 120 mm.

In the face cooling strategy, the cell has a large surface area for cooling and a minimum normal distance from the cooling plate to the cell. The face cooling concept has the lowest temperature gradient than the other two concepts. Figure-17 show cell normal distance vs. temperature gradient plot for face cooling concept.

For the face cooling concept, the cell normal distance is 29 mm the cell temperature gradient less than 1 °C was observed.

The 1D tool developed was validated for multiple conditions. The cell temperature values from the 1D tool correlated well with the simulated temperature gradient as shown in Table-6

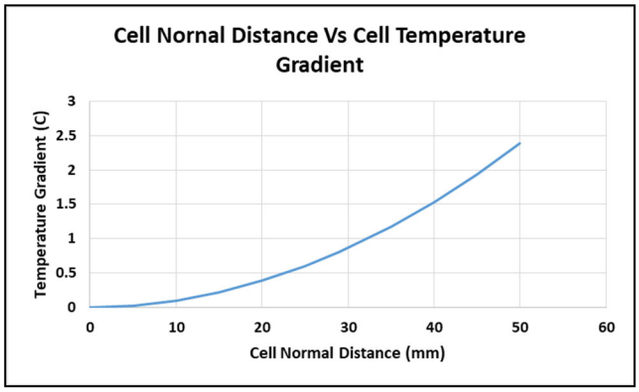


**Fig. 17.**Normal Distance Vs Cell Temperature Gradient for face cooling.

TABLE 6

Cell Temperature Gradient Simulation Vs 1d Prediction.

| Results | Heat Source 1.5 Watt | Heat Source 2.0 Watt | Heat Source 2.75 Watt |
|---|---|---|---|
| Simulated Gradient (C ) | 1.84 | 2.463 | 3.387 |
| Predicted Gradient (C ) | 1.85 | 2.46 | 3.39 |
| % Difference | 0.43 | 0.02 | 0.02 |

Table-7 shows the cell benchmark data of different EVs. The benchmark data show the most of the cell use the bottom cool strategy and have the cell normal distance less than 110 mm. For cells with aspect ratio more than one the bottom cooling strategy is recommended. For cells with aspect ratio less than one the side cooling strategy is recommended.

TABLE 7

Cell Benchmark Data.

| Sr. No. | Vehicle | Cell height (mm) | Cell thickness (mm) | Cell Length (mm) | Aspect Ratio | Weight |
|---|---|---|---|---|---|---|
| 1 | Concept | 216 | 29.2 | 135 | 0.6 | 1790 |
| 2 | GM Bolt | 110 | 15 | 300 | 2.7 | 850 |
| 3 | Jaguar I-Pace | 98 | 12 | 290 | 3.0 | 818 |
| 4 | Audi e-tron | 96 | 12 | 330 | 3.4 | 877 |

## Busbar Location

Reaction heat, Ohmic heat, reversible heat, and external terminal contact resistance heat are the heat sources associated with the operation of Li-ion batteries. The total reversible heat generation is related to cathode and anode entropy changes while the last component of heat is due to the contact resistance between the cell terminals and the external interconnect[4] as shown in Figure-18. Thus, the closer is the busbar with the cooling plate, better it is for the heat dissipation.

## Complexity of Cooling System

As it is well understood, complexity and cost go hand in hand. The face cooling system requires cooling plates after each cell as shown in Figure-19[5]. Hence, the face cooling concept is most complex with multiple connecting parts as compared with bottom and side cooling. In the

bottom and the side cooling, only one cooling plate is required for multiple cells.

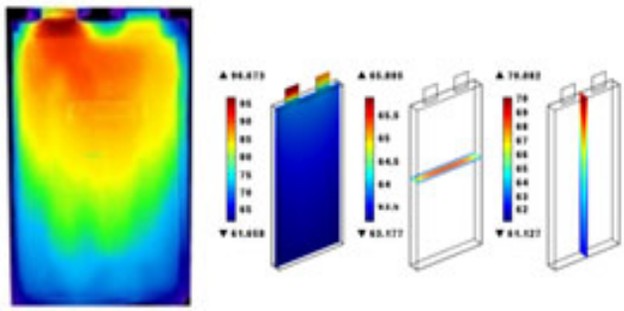

**Fig. 18.**Temperature distribution within the cell.

TABLE 8

Decision matrix of different cooling strategies.

| Sr No | Design Parameter | Bottom Cooling | | Face Cooling | | Side surface cooling | |
|---|---|---|---|---|---|---|---|
| | | Rating | Score | Rating | Score | Rating | Score |
| 1 | Area of cooling | Low | 2 | High | 5 | Medium | **3** |
| 2 | Temperature Gradient | Low | 2 | High | 5 | Medium | 3 |
| 3 | Cell Conductivity | High | 4 | Low | 1 | High | 4 |
| 4 | Cell Busbar Location (Contribute to non uniform heat generation) | Far | 1 | Very close | 5 | Near | 4 |
| 5 | Complexity Of Cooling System (Complex system Can cause leakage) | Less Compl ex | 5 | Compl ex | 1 | Less Complex | 5 |
| 6 | Cost of Cooling System | Inexpe nsive | 5 | Expen sive | 1 | In-expensive | 5 |
| 7 | Cell Normal Distance (<110 mm) | more | 1 | less | 5 | average | 3 |
| | | Total | 20 | Total | 23 | Total | 27 |

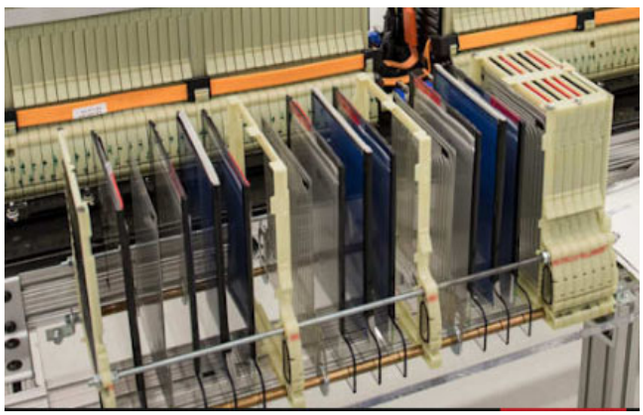

**Fig.19.**Example of face cooling strategy.

### Decision Matrix

Based on all the design parameters, a decision matrix was prepared, which is shown in Table-8. The overall score is in the range of 0 to 5 and for each decision matrix parameter, a score was given. The individual score summation was done. For the current battery pack design layout and cell arrangement, the side cooling concept gets a better overall score.

## Conclusions

Based on the design analysis and 1D & 3D simulation studies, the following conclusions can be drawn:

1) The side cooling seems to be the most efficient and feasible option for the battery pack we developed as it not only offers maximum cooling area but also min temp gradient across the cell.
2) The side cooling concept is the least complex compared to other options.
3) For heat generation of 2.75 Watt and for cell normal distance of 120 mm, temp gradient can still be limited to max $1.0^0$C
4) A close correlation between CFD results and empirical calculations was obtained for temperature gradient values across the cell (deviation max = 0.43%)

### Future Scope

The cells generate more heat near the current collector tab. The temperature distribution is not uniform in the cell. A further study is in progress to estimate the non-uniform heat generation and its effects on the temperature gradient.

### Acknowledgments

Authors would like to express our gratitude to both Mr. Shailesh Saraph and Mr. Srikumar Vaidya, Tata Technologies Ltd., for encouraging us to publish this work.

## References

[1] Satyam Panchal, Scott Mathewson, Roydon Fraser "Measurement of Temperature Gradient and Temperature Response of a Prismatic Lithium-Ion Pouch Cell with LiFePO 4 Cathode Material", March-2017, https://www.researchgate.net/

[2] Addressing the Impact of Temperature Extremes on Large Format Li-Ion Batteries for Vehicle Applications, Ahmad Pesaran, Shriram Santhanagopalan, Gi-Heon Kim, March-2013 https://www.nrel.gov/docs/fy13osti/58145.pdf

[3] Anna Tomaszewska, Zhengyu Chu, "Lithium-ion battery fast charging A review", August-2019, https://www.researchgate.net/

[4] L.H. Saw, A. A. O. Tayand L. Winston Zhang, "Thermal Management of Lithium-ion Battery Pack with Liquid Cooling",March-2015,https://www.researchgate.net/

[5] General Motors Chevrolet Volt Battery Pack Witout Cover March-2015,https://www.autoblog.com/2015/06/13/gm-stationary-battery-plan/

**Address correspondence to:** Yogesh P Dol, *Tata Technologies Ltd. Plot No. 25, Phase 1, Hinjewadi, Rajiv Gandhi Infotech Park, Hinjawadi, Pune, Maharashtra, India. Pin-411057.*
*E-mail: yogesh.dol@tatatechnologies.com*